

Microstructural Evolution of H-BN Matrix Composite Ceramics With Amorphous $\text{La}_2\text{O}_3\text{-Al}_2\text{O}_3\text{-SiO}_2$ Glass Phase During Hot Pressing

Baofu Qiu

Harbin Institute of Technology

Xiaoming Duan (✉ duanxiaoming@hit.edu.cn)

aKey Laboratory of Advanced Structural-Functional Integration Materials & Green Manufacturing Technology, Harbin Institute of Technology, Harbin, 150001, China bInstitute for Advanced Ceramics, School of Materials Science and Engineering, Harbin Institute of Technology, Harbin, 150001, China cState Key Laboratory of Advanced Welding and Joining, Harbin Institute of Technology, Harbin, 150001, China <https://orcid.org/0000-0002-8723-8286>

Zhuo Zhang

Harbin Institute of Technology

Chen Zhao

Harbin Institute of Technology

Bo Niu

Harbin Institute of Technology

Peigang He

Harbin Institute of Technology

Delong Cai

Harbin Institute of Technology

Lei Chen

Harbin Institute of Technology

Zhijia Yang

Harbin Institute of Technology

Yujin Wang

Harbin Institute of Technology

Dechang Jia

Harbin Institute of Technology

Yu Zhou

Harbin Institute of Technology

Keywords: h-BN matrix composite ceramics, Amorphous La₂O₃-Al₂O₃-SiO₂ glass phase, Microstructural evolution, Nanocrystalline precipitation, Mechanical properties

Posted Date: September 14th, 2020

DOI: <https://doi.org/10.21203/rs.3.rs-74072/v1>

License:  This work is licensed under a Creative Commons Attribution 4.0 International License.

[Read Full License](#)

Abstract

BN-La₂O₃-Al₂O₃-SiO₂ composite ceramics were fabricated by hot press sintering using h-BN, La₂O₃, Al₂O₃ and amorphous SiO₂ as the raw materials. The effects of sintering temperature on the microstructural evolution, bulk density, apparent porosity, and mechanical properties of h-BN composite ceramics were investigated. The results indicated that ternary La₂O₃-Al₂O₃-SiO₂ liquid phase was formed during sintering process, which provided an environment for the growth of h-BN grains. With increasing sintering temperature, the cristobalite phase precipitation and h-BN grain growth occurred at the same time, which had the significant influence on the densification and mechanical properties of h-BN composite ceramics. The best mechanical properties of BN-La₂O₃-Al₂O₃-SiO₂ composite ceramics were obtained under sintering temperature of 1700 °C, and the elastic modulus, flexural strength, and fracture toughness were 80.5 GPa, 266.4 MPa and 3.25 MPa·m^{1/2}, respectively.

1. Introduction

Hexagonal Boron Nitride (h-BN) and its matrix composite ceramics are typical structural-functional ceramics that have been widely used in many fields, such as aerospace, machinery, metallurgy, energy, and electronics [1–7]. Compared with Alumina, Zirconia, Silicon Carbide, Silicon Nitride ceramic which have the high hardness and high strength, h-BN presents the relatively low hardness and good machinable properties, because of its hexagonal layered crystal structure similar to that of graphite [8–11]. Furthermore, h-BN ceramics are difficult to sintering densification, so the low melting point sintering additives and/or second phase are usually added to improve the properties of h-BN composite ceramics [12–16].

There have been some researches on the microstructural evolution during sintering and the properties of h-BN ceramics [17–21]. Zhuo Zhang et al. obtained h-BN powders composed of amorphous and nanocrystalline BN by ball milling, and then sintered them under different temperatures and pressures. Higher sintering pressure was more favorable to the preferred orientation growth of the in-plane direction of h-BN grains along the pressure direction, and higher sintering temperature promoted the mass transfer and grain growth. They referred that the structural fluctuation of amorphous BN resulted in the t-BN phase formation during the sintering process, and stacking faults usually existed in the as-grown h-BN grains [22]. Haotian Yang et al. discovered a method on low temperature self-densification of bulk h-BN. During the sintering process, cubic boron nitride (c-BN) particles incorporated into the h-BN flake powders transformed into BN onions with a volume increase, thus filling in voids among the h-BN flakes and densifying the h-BN bulks, finally the dense bulk h-BN with 97.6% theoretical density was achieved by SPS sintering under 1700 °C [23].

For h-BN matrix composite ceramics, there also have been some research results which can reveal the microstructures changing mechanisms [24–28]. Bo Niu et al. investigated the effects of raw h-BN particle size on the textured microstructures of BN-MAS (magnesium aluminosilicate) composite ceramics. With the increase of raw h-BN particle size, h-BN grains tended to orientate with the direction perpendicular to

the hot pressing direction, while the densification effect of MAS phase on BN-MAS composite ceramics decreased with increasing raw h-BN particle size due to the uneven dispersion of MAS phase [26, 29]. Delong Cai et al. researched the influence of sintering process on the BN-MAS composite ceramics. The sintering pressure had a great influence not only on the mechanical properties of composite ceramics, but also on the crystallization of MAS and structural order of h-BN. The nucleophilic attack of N on M (M = Mg^{2+} , Al^{3+} and Si^{4+}) and the electrophilic attack of B on O were the crucial factors on the formation of amorphous MAS phase. In addition, chemical bonding was formed between h-BN and MAS and the matrix atoms diffused into the h-BN layer, leading to a strong bonding interface [30–32].

Ternary amorphous La_2O_3 - Al_2O_3 - SiO_2 glass phase have been reported on promoting sintering densification and improving the room/elevated-temperature mechanical properties of h-BN matrix composite ceramics [33–37]. But the microstructural evolution during sintering process and its effect on properties of this material systems have not been fully revealed yet, which also has important implications for guiding the composition design and process optimization of composite ceramics.

In this study, BN- La_2O_3 - Al_2O_3 - SiO_2 composite ceramics were sintered under different temperatures from 1500 °C to 1900 °C, meanwhile the phase composition, nanocrystalline precipitation and grain growth were systematically investigated. The corresponding mechanical properties were tested to reveal the influence of microstructural evolution on the performance of composite ceramics.

2. Materials And Methods

2.1. Materials fabrication

Commercial powders of h-BN (99.5%, 0.3 μm), hexagonal La_2O_3 (99.9%, 1.0 μm), rhombohedral Al_2O_3 (> 98%, 1.5 μm), and amorphous SiO_2 (99.9%, 3.5 μm) were used as the raw materials. The volume ratio of h-BN: (La_2O_3 - Al_2O_3): SiO_2 was 70:10:20, the mole ratio of La_2O_3 to Al_2O_3 was 1:2.

The weighed powders were mixed with Al_2O_3 balls and ethanol medium for 12 h. The obtained slurry was dried, and then passed through a 100 mesh sieve. The mixed powders were put into a graphite die and cold-compacted uniaxially under 5 MPa pressure. The obtained green compacts were hot press sintered at different temperatures (1500 °C, 1600 °C, 1700 °C, 1800 °C, 1900 °C) for 1 h under 20 MPa with N_2 atmosphere. The heating rate was $15\text{ }^\circ C \cdot \text{min}^{-1}$, and the samples cooled down to room temperature in the furnace spontaneously.

2.2. Materials characterization

Phase compositions were identified by X-ray diffractometer (XRD, D/max- γB CuK α , Rigaku Co., Japan) with a scanning speed of $4\text{ }^\circ \cdot \text{min}^{-1}$. The detailed microstructures were investigated by transmission electron microscope (TEM, Talos F200X, FEI Co., USA). The bulk densities and apparent porosities of samples were measured by Archimedes drainage method. Flexural strength was measured by three-point

bending method using a universal testing machine (Instron-5569, USA), meanwhile Young's modulus was obtained through the stress-strain curve. The sample size was 3 mm × 4 mm × 36 mm with a span of 30 mm and the crosshead speed was 0.5 mm·min⁻¹. Fracture toughness was measured using the single edge notched beam (SENB) method. The sample size was 2 mm × 4 mm × 20 mm with a notch of 2 mm, and the crosshead speed was 0.05 mm·min⁻¹. Fracture morphology was observed using scanning electron microscope (SEM, NanoLab 600i, FEI Co., USA).

3. Results And Discussion

Figure 1(a) presents the X-ray diffraction patterns of BN-La₂O₃-Al₂O₃-SiO₂ composite ceramics sintered under different temperatures. There were only obvious diffraction peaks corresponding to h-BN phase, whereas the diffraction peaks of La₂O₃, Al₂O₃, SiO₂ and their possible reaction products were not found. Considering the total volume content of the adding La₂O₃-Al₂O₃-SiO₂ was about 30%, which had exceeded the minimum threshold of XRD detection. Thus, we inferred that the amorphous glass phase was formed during hot press sintering process, which was difficult to be characterized by XRD.

Comparing with the peaks of h-BN in different composite ceramics, with the increase of sintering temperature, the relative peak intensity of corresponding (002) lattice plane increased gradually. Graphitizing Index (GI) is an indicator of crystallization degree of graphite and similar crystalline structure materials [38], and it is calculated by the following formula:

$$GI = \frac{\text{Area}(100) + \text{Area}(101)}{\text{Area}(102)} \quad (1)$$

where Area(100), Area(101) and Area(102) denote the integral intensity of the corresponding (hkl) reflex of h-BN. Theoretically, the GI value of ideal h-BN crystal is about 1.6, and a higher GI value indicates a greater disorder degree in crystal.

Figure 1(b) shows the calculated GI values of h-BN grains in composite ceramics. With the increase of sintering temperature, GI values showed a decreasing trend, which basically conformed to the change rule of exponential function. From 1500 °C to 1700 °C, the GI values decreased rapidly from 13.7 to 3.4, while from 1700 °C to 1900 °C, the GI values decreased slowly from 3.4 to 2.4. Sintering temperature had a significant influence on the crystallization growth of h-BN in composite ceramics. Higher sintering temperature was conducive to heat and mass transfer in liquid phase environment and the better h-BN grains growth during hot press sintering.

In Fig. 2(a-c), TEM characterization was used to investigate the detail microstructures of BN-La₂O₃-Al₂O₃-SiO₂ composite ceramics hot pressed under 1500 °C, 1700 °C, 1900 °C, and the corresponding element distributions of B, N, O, Al, Si, La were shown in Fig. 2(d). The h-BN grains showed typical lamellar morphology and were uniformly dispersed in the all composite ceramics. La₂O₃-Al₂O₃-SiO₂ phase filled in

the space between h-BN grains and had a good combination with h-BN grains, and there were few obvious interfacial cracks. It could be obviously observed that the grain size of h-BN became bigger with increasing sintering temperature, which was because the liquid phase had better heat and mass transfer effect at higher temperature, promoting the growth of h-BN grains.

Some pores were observed in the sample sintered at 1500 °C, this was due to the relatively low fluidity of the liquid phase at this sintering temperature, which could not fully fill the gaps between the h-BN grains. While in the sample sintered at 1900 °C, a small number of pores were also found, this was because the grown h-BN grains overlapped each other to form closed pores, which could not be filled by liquid phase. By contrast, no obvious pores were found in the sample sintered at 1700 °C, indicating this sintering temperature was favorable for obtaining composite ceramics with the high relative density.

Interface microstructures between h-BN grains and $\text{La}_2\text{O}_3\text{-Al}_2\text{O}_3\text{-SiO}_2$ phase of composite ceramics sintered under different temperatures are presented in Fig. 3(a-c), and the corresponding elemental line scanning profiles from h-BN zone to $\text{La}_2\text{O}_3\text{-Al}_2\text{O}_3\text{-SiO}_2$ zone are shown in Fig. 3(d-f). No defects such as crack could be observed at the phase boundary, indicating a good wettability between $\text{La}_2\text{O}_3\text{-Al}_2\text{O}_3\text{-SiO}_2$ amorphous phase and h-BN grains. The changes of elemental contents were continuous, La, Al, Si and O content of amorphous phase increased, whereas B and N content of h-BN phase decreased gradually along the arrow direction. Comparing with three samples, when the sintering temperature increased from 1500 °C to 1900 °C, the width of the diffusion zone at the two phases interface increased from about 38 nm to more than 55 nm, indicating higher sintering temperature were more beneficial to the element diffusion in the phase interface region during hot press sintering process. In Fig. 3(g), high-resolution transmission electron microscopy (HRTEM) results exhibited the detailed interface zone formed by atom diffusion between $\text{La}_2\text{O}_3\text{-Al}_2\text{O}_3\text{-SiO}_2$ phase and h-BN phase, which showed a gradual transition from order to disorder arrangement. On the whole, continuous, defect-free and interdiffusion grain boundary was beneficial to provide the good interface bonding and better performance of composite ceramics.

Precipitation nanocrystalline was also found in $\text{La}_2\text{O}_3\text{-Al}_2\text{O}_3\text{-SiO}_2$ phase, and with the increase of sintering temperature, the size of these precipitated grains showed a gradual increasing trend, as shown in Fig. 4(a-c). High sintering temperature was more likely to form precipitation phase with bigger size. Through selecting electron diffraction analysis as shown in Fig. 4(d), the precipitated phase was identified as cristobalite, which meant the precipitated cristobalite phase and amorphous $\text{La}_2\text{O}_3\text{-Al}_2\text{O}_3\text{-SiO}_2$ glass phase were coexisted in the composite ceramics.

Figure 5 shows the bulk densities and apparent porosities of BN- $\text{La}_2\text{O}_3\text{-Al}_2\text{O}_3\text{-SiO}_2$ composite ceramics sintered under different temperatures. With the increase of sintering temperature, bulk density of h-BN composite ceramics first increased and then decreased, whereas apparent porosity exhibited the opposite tendency. The composite ceramic sintered at 1700 °C had the highest bulk density and the lowest apparent porosity. With the increase of sintering temperature, the liquid phase had better fluidity and wettability, and could well fill into the voids formed by the overlap of h-BN grains, which contributed to the improvement of densification. However, with the further increase of sintering temperature, h-BN grains

had obvious growth, which led to the larger pores in the mutual framework by the large h-BN grains, resulting in the decrease of relative density.

Figure 6 shows mechanical properties of BN-La₂O₃-Al₂O₃-SiO₂ composite ceramics sintered under different temperatures, including flexural strength, elastic modulus, and fracture toughness. With the increase of sintering temperature, the mechanical properties presented a small increase and followed by a rapid decrease, which was consistent with the tendency of bulk density. The best mechanical properties of BN-La₂O₃-Al₂O₃-SiO₂ composite ceramics were obtained under sintering temperature of 1700 °C, and the elastic modulus, flexural strength, and fracture toughness were 80.5 GPa, 266.4 MPa and 3.25 MPa·m^{1/2}, respectively.

Fracture morphology of BN-La₂O₃-Al₂O₃-SiO₂ composite ceramics sintered under different temperatures are shown in Fig. 7(a-e). The grain size increased significantly with increasing sintering temperature, and the statistically average values are listed in Fig. 7(f). As the sintering temperature changed from 1500 °C to 1900 °C, the average size of h-BN grains increased from 0.35 μm to 2.5 μm. In addition, some pores with the size of several micrometers were found in the fracture morphology of the samples sintered at 1800 °C and 1900 °C, which was caused by the overlap structure of large h-BN grains. In contrast, the samples sintered at relatively low temperatures did not show the obviously large pores.

From the above results, we comprehensively analyzed the influence of sintering temperature on the mechanical properties of BN-La₂O₃-Al₂O₃-SiO₂ composite ceramics, which mainly included the following two points: (1) High sintering temperature facilitated heat transfer and atom diffusion in liquid phase, which were beneficial to liquid phase pore filling to increase the relative density and improve the mechanical properties; (2) The grain sizes of h-BN increased rapidly with the increase of sintering temperature, and when h-BN grains grew to larger size, the porosity of composite ceramics became higher, resulting in an adverse effect on the densifying process and mechanical properties.

The microstructural evolution process of BN-La₂O₃-Al₂O₃-SiO₂ composite ceramics during hot press sintering can be illustrated as Fig. 8 shown. Firstly, the four raw powders were uniformly mixed and heated gradually in the graphite mold (Fig. 8(a)); When the sintering temperature increased, La₂O₃-Al₂O₃-SiO₂ liquid phase was formed and h-BN grains were uniformly distributed in the liquid phase environment (Fig. 8(b)); With the further increase of sintering temperature, the heat and mass transfer ability of the liquid phase was enhanced, and the h-BN grains began to grow significantly. At the same time, the cristobalite phase nanocrystalline was also precipitated in the liquid phase (Fig. 8(c)); At the case of sintering temperature increasing or holding time extending, the grain size of h-BN and precipitated cristobalite phase continued growing, and finally the h-BN, cristobalite and amorphous phase were coexisted in the sintered BN-La₂O₃-Al₂O₃-SiO₂ composite ceramics (Fig. 8(d)).

4. Conclusions

The BN-La₂O₃-Al₂O₃-SiO₂ composite ceramics were hot press sintered under different temperatures to reveal the microstructural evolution mechanisms. Ternary La₂O₃-Al₂O₃-SiO₂ liquid phase was formed during the sintering process, which had a good wettability with h-BN grains and could effectively fill the pores to improve the densification of composite ceramics. Higher sintering temperature contributed to the growth and crystallization of h-BN grains through better heat transfer and atomic diffusion in liquid phase environment. Furthermore, cristobalite nanocrystals were precipitated from the liquid phase and also grow gradually with the increase of sintering temperature. The BN-La₂O₃-Al₂O₃-SiO₂ composite ceramics sintered under 1700 °C exhibited the best mechanical properties, which was attributed to the mutual influence of liquid phase environment, h-BN grain size and precipitated phase.

Declarations

Acknowledgments

This study was financially supported by the National Key Research and Development Program of China (No. 2017YFB0703200) and the National Natural Science Foundation of China (Nos. 51672060, 51832002 and 51372050).

References

1. Eichler J, Lesniak C (2008) Boron nitride (BN) and BN composites for high-temperature applications. *J Eur Ceram Soc* 28:1105–1109
2. Lipp A, Schwetz KA, Hunold K (1989) Hexagonal boron nitride: fabrication, properties and applications. *J Eur Ceram Soc* 5:3–9
3. Perevislov SN, *Slabov VS, Panteleev IB* et al. Chemical resistance of liquid-phase-sintered materials based on Si₃N₄-BN. *Glass Ceram* 2020, 76: 451–456.
4. Greil P (2002) Advanced engineering ceramics. *Adv Eng Mater* 4:247–254
5. Chen JJ, Chen JX, Wang S, Yang J (2020) Tribological properties of h-BN matrix solid-lubricating composites under elevated temperatures. *Tribol Int* 148:106333
6. Yadav V, Kulshrestha V (2019) Boron nitride: a promising material for proton exchange membranes for energy applications. *Nanoscale* 11:12755–12773
7. Li YZ, Chen F, Li XY, Shen Q, Zhang LM (2020) Addition of h-BN for enhanced machinability and high mechanical strength of AlN/Mo composites. *Ceram Int* 46:20097–20104
8. Smith EA (1971) Graphite and boron nitride ("white graphite"): aspects of structure, powder size, powder shape, and purity. *Powder Metall* 14:110–123
9. Fang HM, Bai SL, Wong CP (2016) "White graphene"-hexagonal boron nitride based polymeric composites and their application in thermal management. *Compos Commun* 2:19–24
10. Ooi N, Rairkar A, Lindsley L, Adams JB (2006) Electronic structure and bonding in hexagonal boron nitride. *J Phys Condens Mat* 18:97–115

11. Ci LJ, Song L, Jin CH et al (2010) Atomic layers of hybridized boron nitride and graphene domains. *Nat Mater* 9:430–435
12. Duan XM, Yang ZH, Chen L et al (2016) Review on the properties of hexagonal boron nitride matrix composite ceramics. *J Eur Ceram Soc* 36:3725–3737
13. Zhang GJ, Zou J, Ni DW, Liu HT, Kan YM (2012) Boride ceramics: densification, microstructure tailoring and properties improvement. *J Inorg Mater* 27:225–233
14. Taylor KM (1955) Hot pressed boron nitride. *Ind Eng Chem* 47:2506–2509
15. Zhang GJ, Yang JF, Ando M, Ohji T (2002) Nonoxide-boron nitride composites: in situ synthesis, microstructure and properties. *J Eur Ceram Soc* 22:2551–2554
16. Marion JE, Hsueh CH, Evans AG (1987) Liquid-phase sintering of ceramics. *J Am Ceram Soc* 70:708–713
17. Duan XM, Jia DC, Wang Z et al (2016) Influence of hot-press sintering parameters on microstructures and mechanical properties of h-BN ceramics. *J Alloy Compd* 684:474–480
18. Zhang X, Chen JX, Li XC et al (2015) Microstructure and mechanical properties of h-BN/Y₂SiO₅ composites. *Ceram Int* 41:1279–1283
19. Gao XJ, Yan DM, Cao JW et al (2015) The study on the property and the microstructure of pressureless sintered h-BN ceramics. *Adv Mater Res* 1104:9–14
20. Zhang ZT, Teng LD, Li WC (2007) Mechanical properties and microstructures of hot-pressed MgAlON-BN composites. *J Eur Ceram Soc* 27:319–326
21. Chen JJ, Chen JX (2020) Formation and thermal stability of dual glass phases in the h-BN/SiO₂/Yb-Si-Al-O composites. *J Eur Ceram Soc* 40:456–462
22. Zhang Z, Duan XM, Qiu BF et al (2020) Microstructure evolution and grain growth mechanisms of h-BN ceramics during hot-pressing. *J Eur Ceram Soc* 40:2268–2278
23. Yang H, Yang HT, Fang HL et al (2019) Low temperature self-densification of high strength bulk hexagonal boron nitride. *Nat Commun* 10:1–9
24. Tian Z, Wang Y, Zhang Z et al (2020) The effects of holding time on grain size, orientation degree and properties of h-BN matrix textured ceramics. *Mater Chem Phys* 248:122916
25. Duan XM, Jia DC, Wu ZL et al (2013) Effect of sintering pressure on the texture of hot-press sintered hexagonal boron nitride composite ceramics. *Scripta Mater* 68:104–107
26. Zhang Z, Duan XM, Qiu BF et al (2019) Preparation and anisotropic properties of textured structural ceramics: a review. *J Adv Ceram* 8:289–332
27. Qiu BF, Duan XM, Zhang Z et al (2020) Microstructural evolution and mechanical properties of h-BN composite ceramics with Y₂O₃-AlN addition by liquid-phase sintering. *Rare Met* 39:555–561
28. Wei DQ, Meng QC, Jia DC (2007) Microstructure of hot-pressed h-BN/Si₃N₄ ceramic composites with Y₂O₃-Al₂O₃ sintering additive. *Ceram Int* 33:221–226

29. Niu B, Cai DL, Yang ZH et al (2019) Anisotropies in structure and properties of hot-press sintered h-BN-MAS composite ceramics: effects of raw h-BN particle size. *J Eur Ceram Soc* 39:539–546
30. Cai DL, Yang ZH, Duan XM et al (2016) Inhibiting crystallization mechanism of h-BN on α -cordierite in BN-MAS composites. *J Eur Ceram Soc* 36:905–909
31. Cai DL, Yang ZH, Duan XM et al (2016) Influence of sintering pressure on the crystallization and mechanical properties of BN-MAS composite ceramics. *J Mater Sci* 51:2292–2298
32. Cai DL, Yang ZH, Duan XM et al (2015) A novel BN-MAS system composite ceramics with greatly improved mechanical properties prepared by low temperature hot-pressing. *Mater Sci Eng A* 633:194–199
33. Qiu BF, Duan XM, Zhang Z et al (2020) Microstructure and room/elevated-temperature mechanical properties of hot-pressed h-BN composite ceramics with La_2O_3 - Al_2O_3 - SiO_2 addition. *J Eur Ceram Soc* 40:2260–2267
34. Iftekhar S, Grins J, Edén M (2010) Composition-property relationships of the La_2O_3 - Al_2O_3 - SiO_2 glass system. *J Non-Cryst Solids* 356:1043–1048
35. Li L, Tang ZJ (1999) Phase diagram prediction of the Al_2O_3 - SiO_2 - La_2O_3 system. *J Mater Sci Tech* 15:439–443
36. Marchi J, Morais DS, Schneider J et al (2005) Characterization of rare earth aluminosilicate glasses. *J Non-Cryst Solids* 351:863–868
37. Iftekhar S, Grins J, Gunawidjaja PN, Edén M (2011) Glass formation and structure-property-composition relations of the RE_2O_3 - Al_2O_3 - SiO_2 (RE = La, Y, Lu, Sc) systems. *J Am Ceram Soc* 94:2429–2435
38. Lorenz H, Orgzall I (2004) Influence of the initial crystallinity on the high pressure-high temperature phase transition in boron nitride. *Acta Mater* 52:1909–1916

Figures

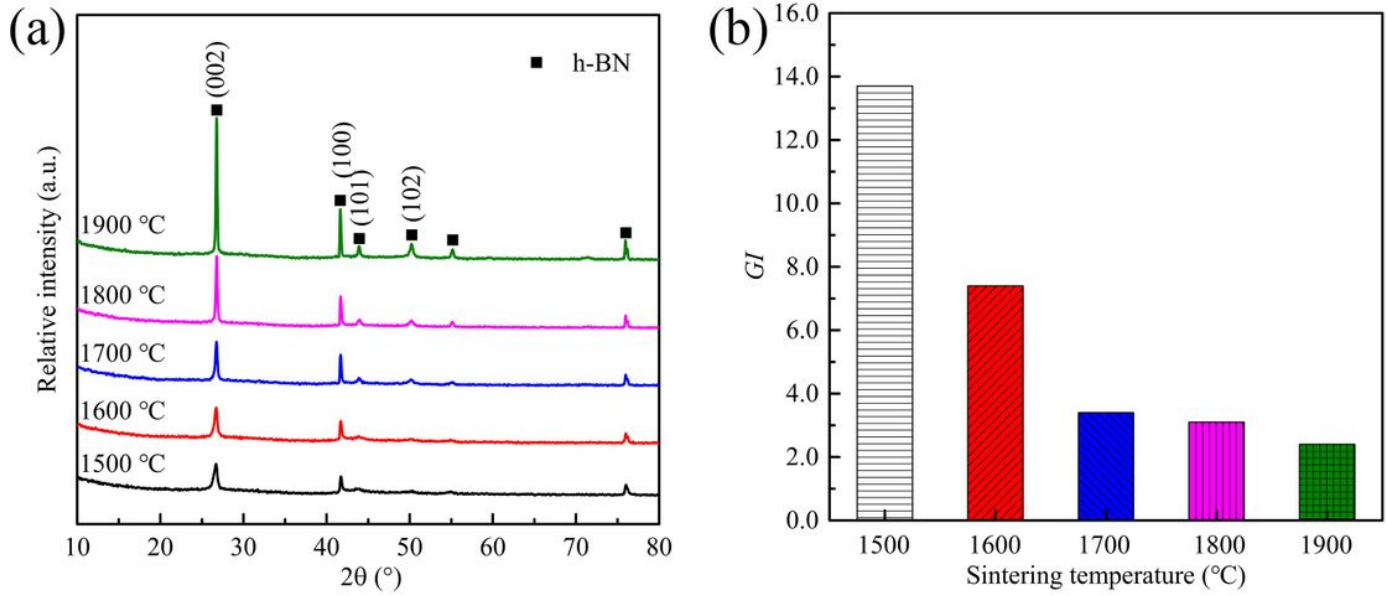


Figure 1

XRD patterns (a) and crystallization graphitization index (b) of BN-La₂O₃-Al₂O₃-SiO₂ composite ceramics.

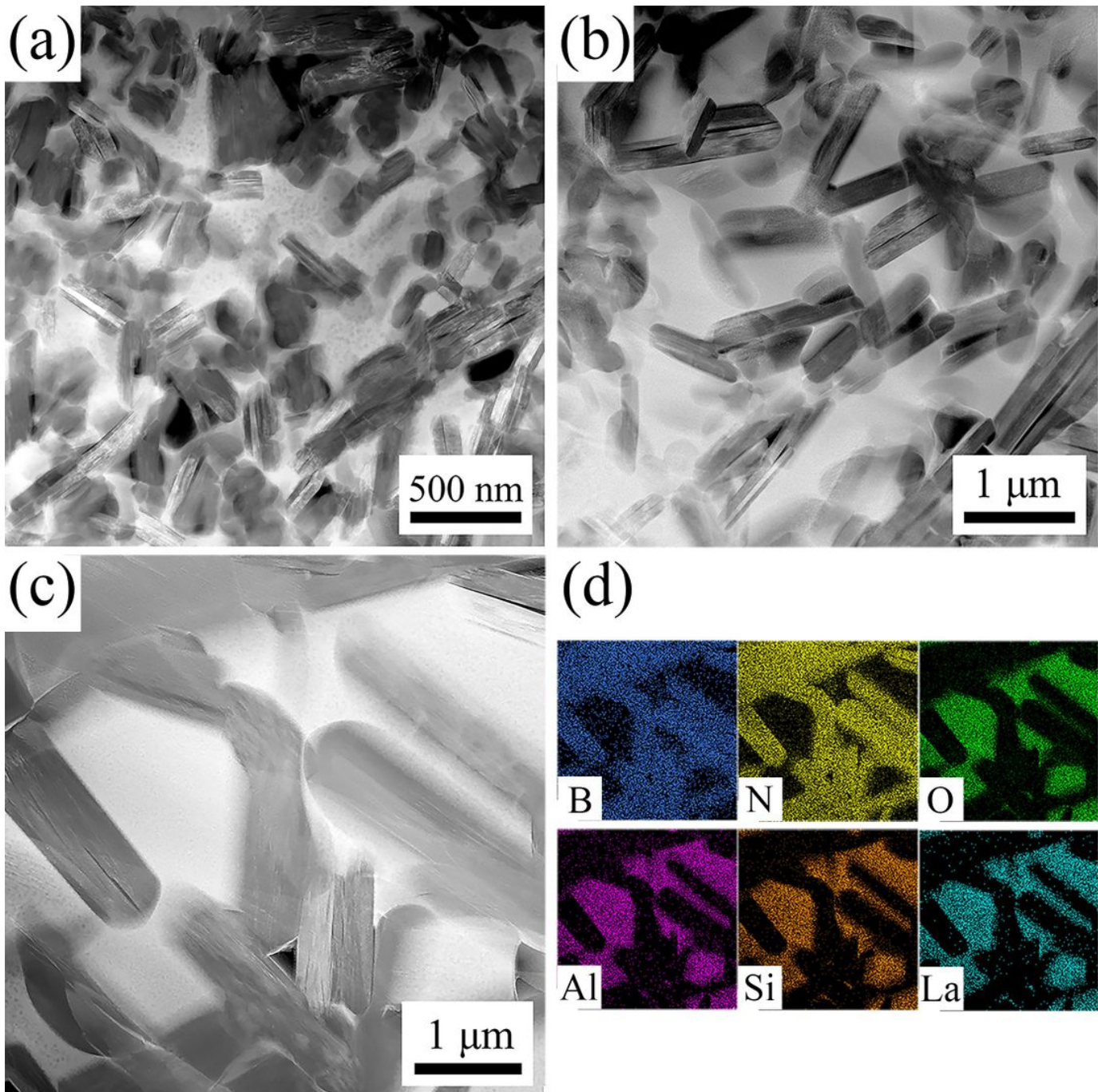


Figure 2

Microstructures of BN-La₂O₃-Al₂O₃-SiO₂ composite ceramics sintered under different temperatures: (a) 1500 °C; (b) 1700 °C; (c) 1900 °C; (d) B, N, O, Al, Si and La element distribution corresponding to (c).

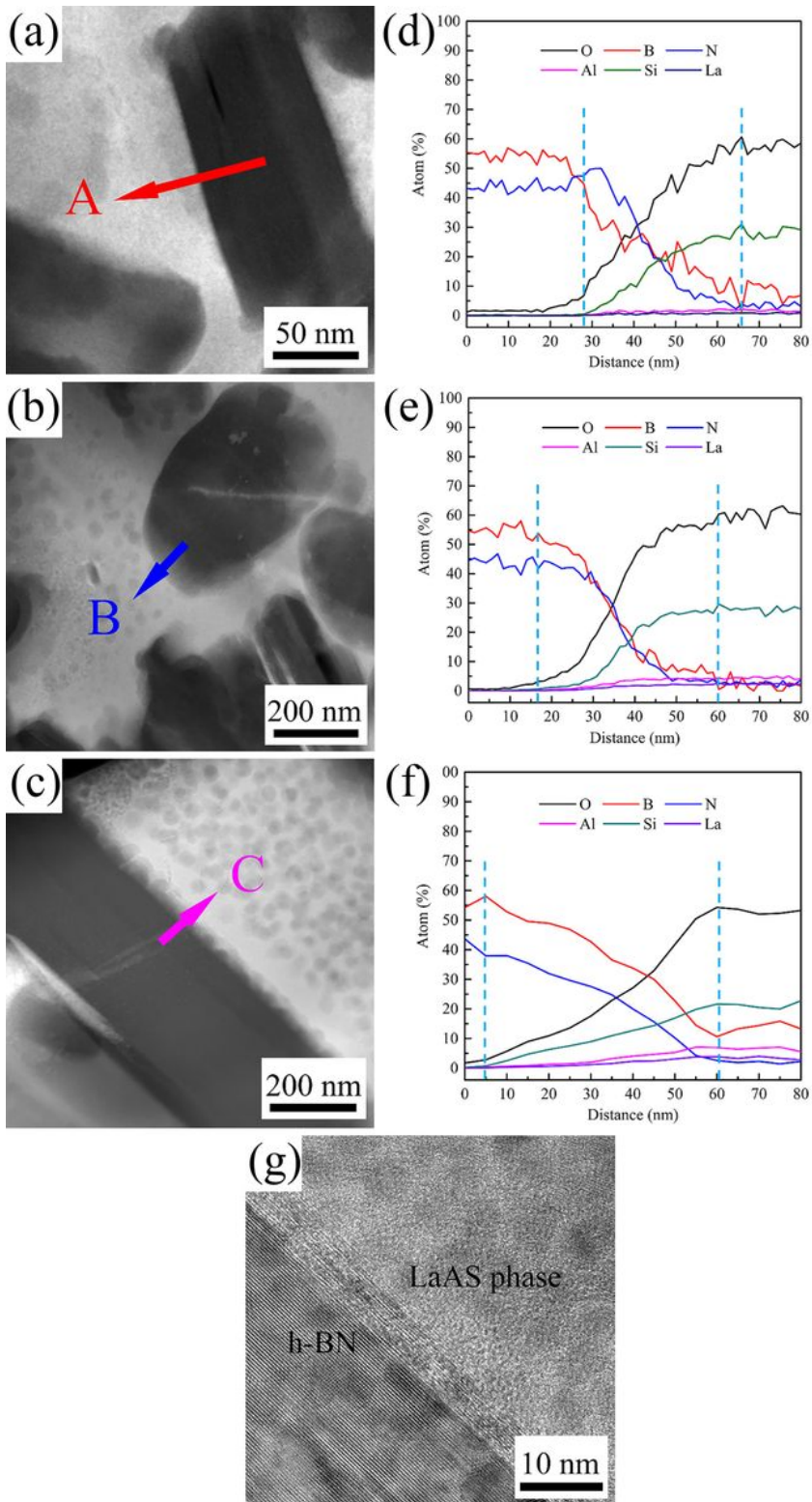


Figure 3

Interface microstructures between h-BN grains and La₂O₃-Al₂O₃-SiO₂ phase of composite ceramics sintered under different temperatures: (a) 1500 °C; (b) 1700 °C; (c) 1900 °C; (d), (e), (f) elemental line scanning corresponding to line A, B, C; (g) HRTEM corresponding to interface of LaAS phase and h-BN grain in (c).

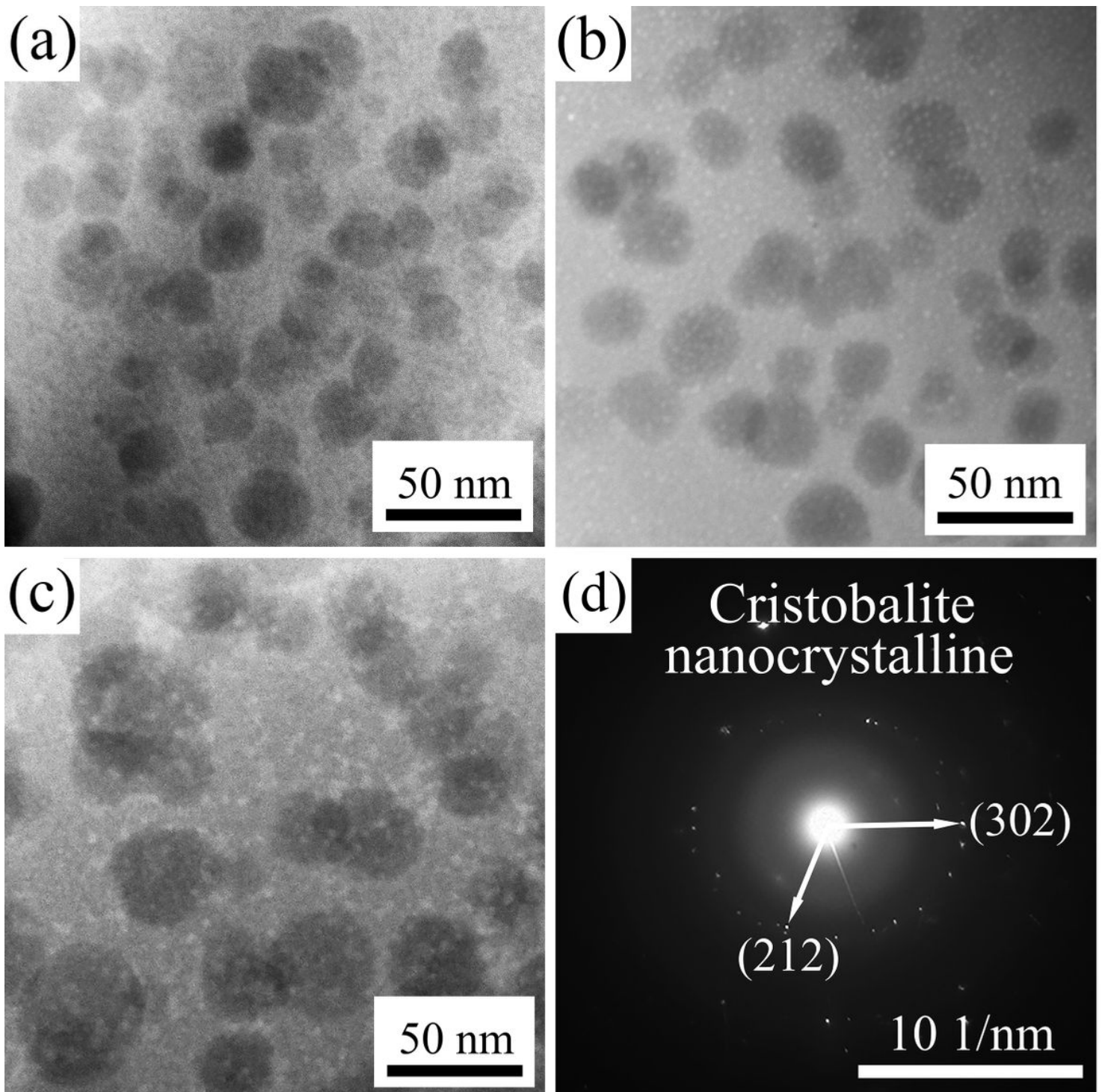


Figure 4

Nanocrystalline precipitation microstructures in $\text{La}_2\text{O}_3\text{-Al}_2\text{O}_3\text{-SiO}_2$ phase of composite ceramics sintered under different temperatures: (a) 1500 °C; (b) 1700 °C; (c) 1900 °C; (d) diffraction patterns of amorphous phase and cristobalite nanocrystalline.

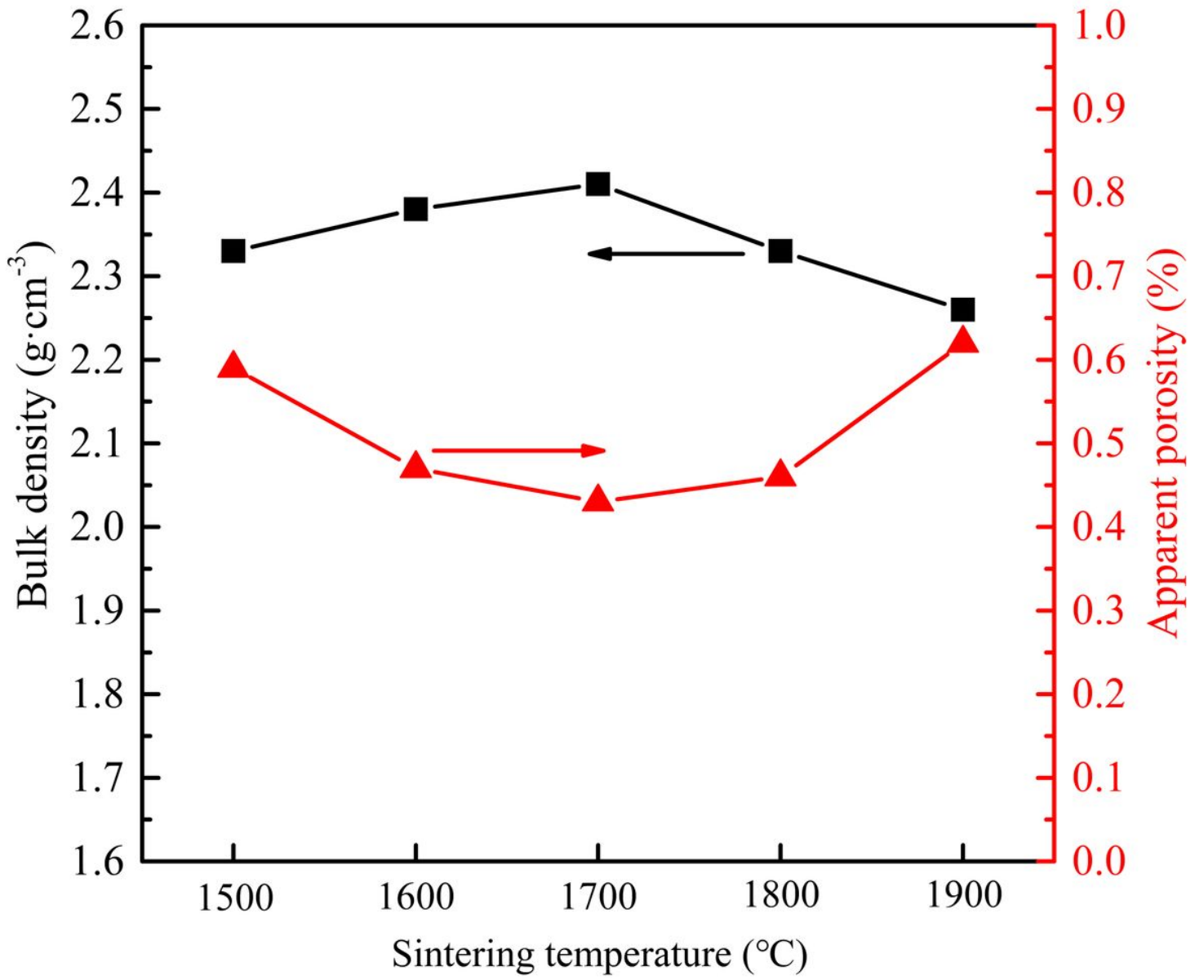


Figure 5

Bulk densities and apparent porosities of BN-La₂O₃-Al₂O₃-SiO₂ composite ceramics.

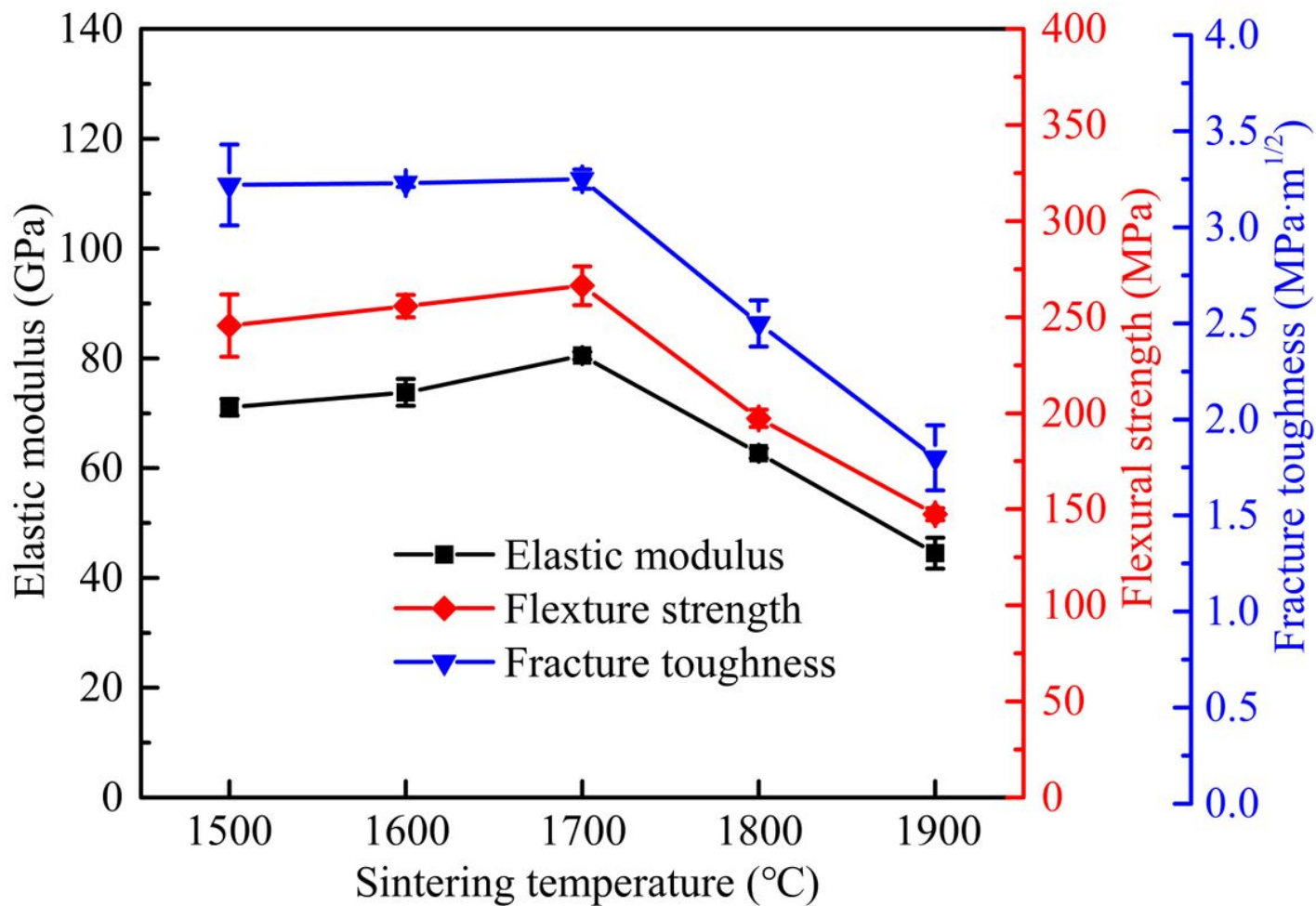


Figure 6

Mechanical properties of BN-La₂O₃-Al₂O₃-SiO₂ composite ceramics.

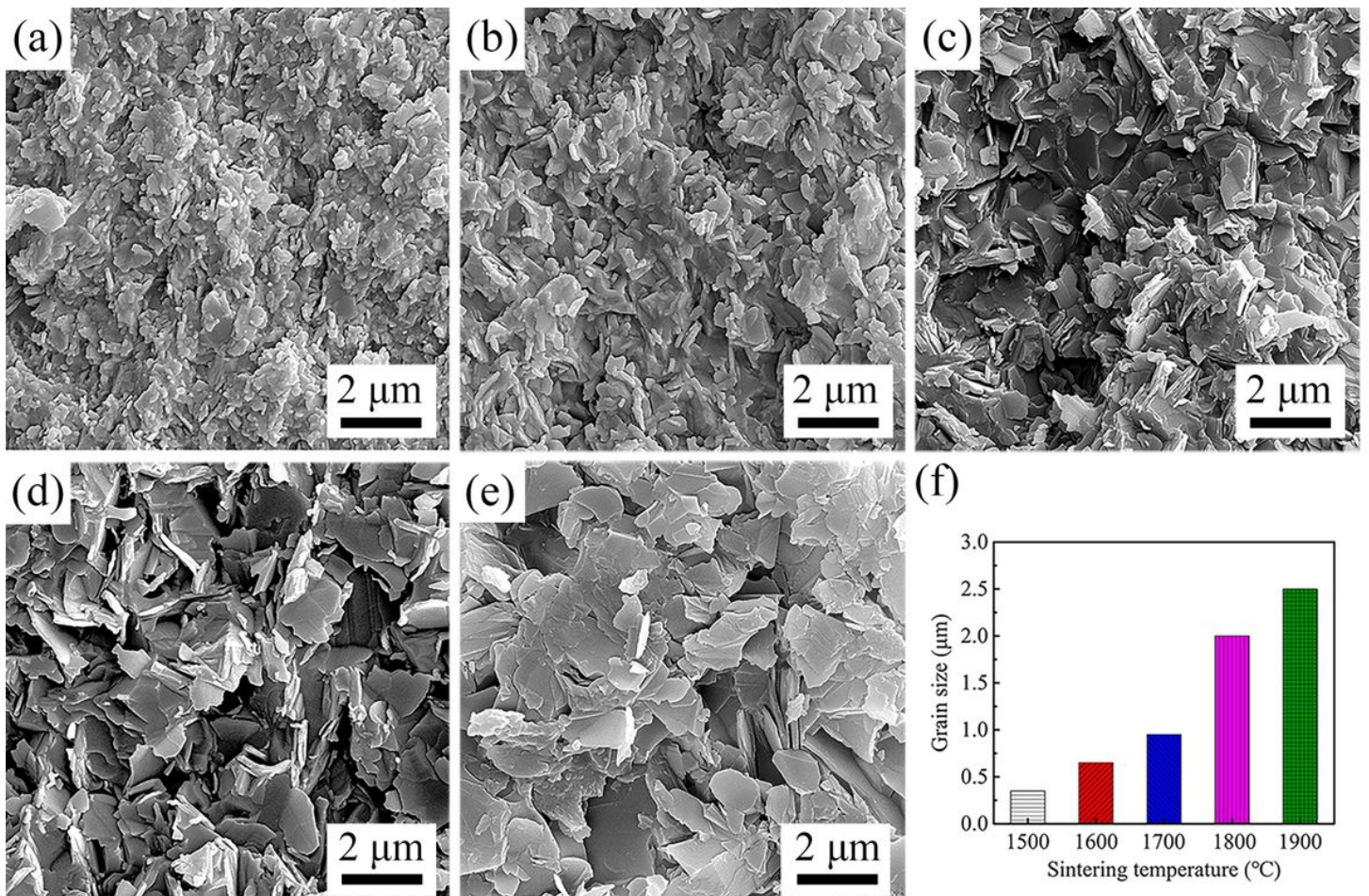


Figure 7

Fracture morphology of BN-La₂O₃-Al₂O₃-SiO₂ composite ceramics sintered under different temperature: (a) 1500 °C; (b) 1600 °C; (c) 1700 °C; (d) 1800 °C; (e) 1900 °C; (f) statistics of average grain size.

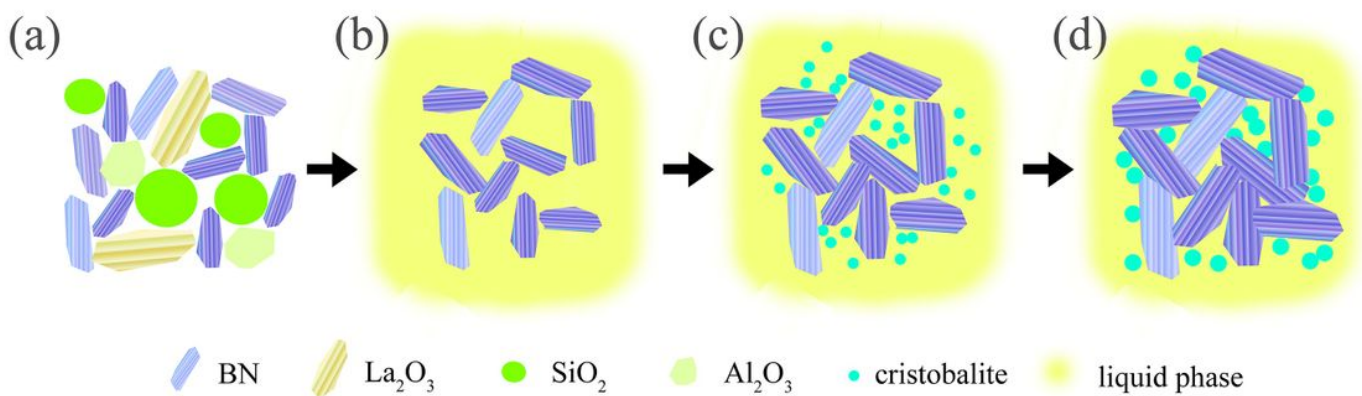


Figure 8

Microstructural evolution mechanism diagrams of BN-La₂O₃-Al₂O₃-SiO₂ composite ceramics.